Cerebral CT Perfusion Using an Interventional C-Arm Imaging System: Cerebral Blood Flow Measurements

A. Ganguly, **A. Fieselmann**, **M. Marks**, **J. Rosenberg**, **J. Boese**, **Y. Deuerling-Zheng**, **M. Straka**, **G. Zaharchuk**, **R. Bammer**, and **R. Fahrig**

From the Department of Radiology (A.G., M.M., J.R., M.S., G.Z., R.B., R.F.), Stanford University, Stanford, California; Pattern Recognition Laboratory (A.F.), Department of Computer Science, and Erlangen Graduate School in Advanced Optical Technologies (A.F.), Friedrich-Alexander University Erlangen-Nuremberg, Erlangen, Germany; and Siemens AG (A.F., J.B., Y.D.-Z.), Healthcare Sector, Forchheim, Germany.

Abstract

BACKGROUND AND PURPOSE—CTP imaging in the interventional suite could reduce delays to the start of image-guided interventions and help determine the treatment progress and end point. However, C-arms rotate slower than clinical CT scanners, making CTP challenging. We developed a cerebral CTP protocol for C-arm CBCT and evaluated it in an animal study.

MATERIALS AND METHODS—Five anesthetized swine were imaged by using C-arm CBCT and conventional CT. The C-arm rotates in 4.3 seconds plus a 1.25-second turnaround, compared with 0.5 seconds for clinical CT. Each C-arm scan had 6 continuous bidirectional sweeps. Multiple scans each with a different delay to the start of an aortic arch iodinated contrast injection and a novel image reconstruction algorithm were used to increase temporal resolution. Three different scan sets (consisting of 6, 3, or 2 scans) and 3 injection protocols (3-mL/s 100%, 3-mL/s 67%, and 6-mL/s 50% contrast concentration) were studied. CBF maps for each scan set and injection were generated. The concordance and Pearson correlation coefficients (ρ and r) were calculated to determine the injection providing the best match between the following: the left and right hemispheres, and CT and C-arm CBCT.

RESULTS—The highest ρ and r values (both 0.92) for the left and right hemispheres were obtained by using the 6-mL 50% iodinated contrast concentration injection. The same injection gave the best match for CT and C-arm CBCT for the 6-scan set ($\rho = 0.77$, $r = 0.89$). Some of the 3-scan and 2-scan protocols provided matches similar to those in CT.

CONCLUSIONS—This study demonstrated that C-arm CBCT can produce CBF maps that correlate well with those from CTP.

Guidelines for early management of ischemic stroke recommend IA therapies for selected patients in addition to or in some cases in place of IV treatment.[1] Imaging-selection criteria by using either CTP or PWI/DWI may allow identification of salvageable tissue. A primary requirement for success in such procedures is that the intervention be conducted as soon as possible after the onset of symptoms, often within 6 hours. However, this physiologic imaging of salvageable tissue represents a "snapshot" of the brain parenchyma before treatment is administered. In addition, reperfusion treatment may take several hours to be completed during which time there is likely to be a change in the perfusion state of the

cerebral tissue. This lessens the relevance and accuracy of the pretherapy CT or MR imaging once treatment has started and the perfusion has been altered.[2]

Tissue perfusion information during and immediately following the recanalization therapy may be helpful. Often post-procedural imaging earlier than 24 hours is undertaken only if symptomatic deterioration occurs. However, there is evidence suggesting that postprocedural reperfusion imaging can provide a good measure of outcome. MR imaging studies demonstrate that patients treated IV with tissue plasminogen activator who achieve early reperfusion within 3–6 hours of therapy and have mismatch have improved outcomes compared with those patients without mismatch.[3] Because the start of the intervention is sometimes delayed and the intervention itself often takes hours to complete, intra- and postprocedural perfusion data could have clinical significance.

Intraprocedural CTP may also be useful for management of hemodynamics during anesthesia (eg, blood pressure and hydration parameters). This is important because some recent studies[4,5] have suggested that general anesthesia may result in poorer outcomes after stroke. It is conceivable that these poorer outcomes could be attributed to hypotension induced during anesthesia.

A recent publication by Ahmed et al[6,7] suggests that the availability of perfusion information in the angiographic suite where the image-guided therapy is conducted could have added value in stroke management. These authors have been able to successfully obtain CBV maps in a canine model by using an angiographic C-arm CBCT system. With a modified injection and reconstruction scheme, the CBV maps obtained were comparable with CT. However, the authors were not able to obtain CBF or MTT and TTP parameter maps because of the limited temporal resolution of the angiographic C-arm systems currently available. The rotation speeds of the C-arms are typically an order of magnitude slower than rotation times in CT. Because these parameter maps are critical for complete perfusion information,[8,9] the usefulness of perfusion data from the C-arm CBCT system can be complete if it provides this information.

We have designed a method that will provide the CBF information directly from C-arm CBCT data. The CBV and MTT can be calculated from the area under the TDC for the CBV, and the ratio of the CBV to CBF provides the MTT.

Materials and Methods

Animal Preparation

We imaged cerebral perfusion in 5 large healthy female swine (54.1 ± 4.7 kg) under institutional review board approval. The animals were imaged on a CBCT system (Axiom Artis dTA and syngo DynaCT; Siemens, Erlangen, Germany) and also underwent CTP scans on a conventional CT scanner. The CTP for 2 animals was performed on a 64-section scanner (Somatom Sensation 64, Siemens), and the other 3 animals were imaged on an 8-section scanner (LightSpeed, GE Healthcare, Milwaukee, Wisconsin). A preanesthetic cocktail of Telazol (tiletamine HCl and zolazepam HCl) 5–7 mg/kg body weight, mixed with atropine, 0.05 mg/kg, into 1 syringe was given rapidly intramuscularly into the neck muscle. Approximately 10 minutes later, the pig was in lateral recumbency and moved to the preparation area where the animal was accurately weighed, then placed on a face mask of isoflurane inhalant gas at 2%–3%, while an IV catheter was placed in the ear vein. When the animal was void of jaw and vagal tone, she was intubated and returned to Isoflurane gas, which was reduced to 1.5%–2% as needed. Constant monitoring of the heart and respiratory rates, body temperature, fluid rate, jaw tone, blood gases, activated clotting time, and saturated oxygen levels was maintained. Following anesthetization and intubation, an IV

catheter was placed, and the animal was mechanically ventilated. Femoral sheaths were placed for venous and arterial access.

Injection Protocol

An iodinated contrast agent (iohexol, 350 mg I/mL, Omnipaque; Nycomed, Princeton, New Jersey) was injected by using a programmable dual-head power injector (Medtron, Saarbrücken, Germany). The contrast agent was delivered IA by using a 5F pigtail catheter (Vanguard; Medrad, Indianola, Pennsylvania) placed at the root of the aortic arch under fluoroscopic guidance.[5]

A DSA run was used to verify that both left and right carotid arteries received approximately equal fractions of the contrast agent. During these test DSA runs, we found that the fraction of iodinated contrast entering the left and right CCAs was sensitive to the location of the catheter tip in the aorta. The location directly impacts the mixing of the contrast with blood, as has been found previously.[10,11] The higher injection rates (6 mL/s compared with 3 mL/s) should provide better mixing before the contrast is washed out. The best location of the catheter was selected after a qualitative analysis of the DSA runs following tests at a few trial locations near the root of the aortic arch. Once the catheter location was found to be satisfactory, the portion of the catheter extending outside the sheath was taped to the skin next to the puncture to prevent gross dislocation.

All studies were performed by using the arterial contrast. The arterial approach was used because the C-arm CBCT system has lower contrast resolution, given that its dynamic range is smaller than that of CT (12 bits padded to 14 versus 20 bits, respectively). Hence an IV injection would need a much higher dose of iodinated contrast when imaged by using the C-arm CBCT system to allow the TDCs to be clearly measurable above the image noise. All injections were 8 seconds in duration. We tested 3 different injection volumes and 2 different injection rates: set 1 = 3 mL/s, 67% dilution; set 2 = 6 mL/s, 50% dilution; set 3 = 3 mL/s, 100% dilution. The maximum total volume of iodinated contrast was kept similar to that used clinically at our institution, which is between 40 and 50 mL. These 3 injections were used to understand whether faster injection rates were better for the same volume of injected contrast and whether diluting the contrast but maintaining the same volume would give similar results, hence reducing the contrast load.

Image-Acquisition Protocol

The primary limitation of the C-arm CBCT system is the slow rotation speed of the C-arm, which, in the imaging system used, is a 4.3-second rotation time per sweep, covering 191° with a 1.25-second turnaround time. Additionally, it can be set up for only 6 consecutive bidirectional scans at a time (DynaCT). Because 1 DynaCT scan set gives a maximum of 6 image volumes, it will result in sparsely sampled TDCs with a total of 5.55 seconds between each image volume. This outcome is expected to lead to errors, particularly in estimating the AIF needed to normalize the perfusion data as is done in standard calculation methods. One DynaCT run with 6 sweeps has an x-ray on-time of 25.8 seconds and a total imaging time of 32.05 seconds because of the finite turnaround time. The CTP scans by using the conventional CT scanner, on the other hand, use rotation times of 0.5 seconds with images acquired every 1 second (as is done clinically to spare dose) for a total of 50 seconds.

To overcome this speed limitation, we developed a targeted imaging scheme for perfusion imaging with the C-arm CBCT. We chose to increase the number of time points at which data were acquired by obtaining multiple DynaCT scans with each set, starting at a different delay with respect to the start of a repeated 8-second bolus of contrast agent. Fig 1 shows an example of this imaging scheme and the associated improvement in the temporal sampling.

A superset of 6 such DynaCT scans (Fig 1*A-F*) was acquired by using the following optimized delays for the start of the scans following each of the 6 contrast injections: −4.6 seconds, −2.8 seconds, −0.9 seconds, +0.9 seconds, +2.8 seconds, and +4.6 seconds. The negative signs indicate that x-ray imaging started before the contrast injection, while positive signs indicate that the scan started after the injection. Between each scan, a baseline image was obtained. This allowed the removal of any existing enhancement from the iodinated contrast already on board following earlier injections.

The total scan length covered during imaging was 150 mm on the C-arm CBCT system because of the availability of the large-area flat panel detector. The coverage was 3 cm on the Somatom and 2 cm on the LightSpeed for the conventional CTP scans.

All imaging on the C-arm CBCT system was performed at 81 kV(peak) with the dose to the detector set at 1.2 μGy per projection. Automatic exposure control was enabled to allow x-ray dose modification during rotation of the C-arm. A baseline image consisting of a single scan was acquired for subtracting the effect of any residual iodinated contrast from previous image acquisitions. For the CTP scans, the CT scanner was set to 80 kVp with a reference milliampere-second of 270 for the Somatom and the LightSpeed. Total imaging time was set to 50 seconds, which included 10 seconds precontrast baseline imaging and 40 seconds of postcontrast imaging. A delay of 4 seconds following the injection of contrast was used because that is the lowest setting allowed on the scanner under the perfusion imaging protocol. The collimations used in the 2 cases were 2.4 and 1.25 mm for the Somatom and LightSpeed, respectively.

Image-Reconstruction Method

The image-acquisition method for C-arm CBCT described above increases the number of sample points along the TDC. Each reconstructed dataset from a single sweep is, however, an average of the dynamics that happen over the 4.3 seconds during which each sweep is completed. Also the projection data acquired during the C-arm CBCT acquisition is irregularly sampled, given the bidirectional sweep with finite turnaround. To compensate for these effects, we use a modified image-reconstruction scheme. The algorithm involves first reorganizing the acquired 2D projection datasets from the 6 scans (each containing data from 6 sweeps) such that the datasets are sequential in time. Reconstruction of the data is based on an extension[12] of the work by Montes[13] and Montes and Lauritsch.[14] Briefly, this involves dividing the data from 1 sweep into several equiangular blocks, which, in our case, were optimized to be 6 blocks. The assumption is that the change of the attenuation values during the time required to scan each block is negligible. Initial backprojection (voxel size $0.5 \times 0.5 \times 0.5$ mm) of the data from each block is performed, followed by temporal interpolation of values between blocks for each voxel, assuming a smooth contrast-induced temporal-enhancement function. In this work, a linear interpolation was used to provide regularly sampled data in intervals of 1 second.

To investigate the possibility of reducing the number of scans below 6, we also reconstructed some subsets of the superset of 6 scans. Reducing the scan number should reduce the x-ray and iodinated contrast dose and the procedure time as well as ease workflow, making the approach clinically relevant. Only those scan combinations that were practical from the point of view of covering a large portion of the TDCs and that sampled the rising part of the curves well were considered. As described before, we denote the x-ray delay times with letters from A to F (A =−4.6 seconds, B =−2.8 seconds, C =−0.9 seconds, D =+0.9 seconds, E =+2.8 seconds, F =+4.6 seconds). The sets of 3 scans analyzed were ABC, ACE, BCD, and BDF; sets of 2 scans considered were AB, AC, AD, BC, and BD; and single scans were A, B, and C.

Image Preprocessing

To minimize the effects of motion-related artifacts, we applied a motion-correction algorithm during image reconstruction on the basis of a registration algorithm that uses mutual information.[15,16] Each time frame was registered onto the first (baseline) image.

The CTP images were initially reconstructed at the highest resolution of $0.4 \times 0.4 \times 2.4$ mm in case of the data from the Somatom and $0.5 \times 0.5 \times 1.25$, from the LightSpeed. This reconstruction was performed to facilitate volume registration between the C-arm CBCT data and the CTP data. Image registration with a rigid transform method was used to orient the C-arm CBCT volume to match the CTP data. Thick sections (typically 10 mm) are used for generating clinical perfusion maps; therefore, following image registration, the sections were binned to 9.6 mm in case of data from the Somatom and 10.0 mm in the case of data from the LightSpeed. This step resulted in 3 reconstructed sections for the first 2 animals and 2 sections for the last 3. To remove any bias in the statistical analysis, we used only 2 sections per animal. The reoriented C-arm CBCT data were also binned into sections of equal thickness to allow direct comparison of perfusion maps.

Perfusion Calculations

We developed CBF map-calculation software in-house instead of using standard software packages.[10] This was done to allow seamless integration into the image-processing pipeline. The CBF maps were computed by using the deconvolution approach.[17,18] For deconvolution, singular-value decomposition with a fixed regularization threshold (20% of the maximum singular value) was applied. The AIF was manually selected from the reconstructed sections. The vessel selected was a branch of the left CCA that supplies blood to the rete mirabile. Obtaining an AIF in arteries downstream from the rete was difficult, particularly in the CTP images because of partial volume effect. Corrections for brain attenuation (1.04 g/mL of tissue) and hematocrit differences of 0.73 (valid for human brain) between large vessels and capillaries were applied. Hence, it was assumed that the maps represented quantitative parameters of perfusion of the subject's brain.

Statistical Analysis

The CBF values for the C-arm CBCT data were compared with the CT results. The dataset consisted of 2 sections per animal for the 5 swine imaged. In every section, circular regions of interest were drawn in each of the 2 hemispheres in the white matter (3 region of interest) and gray matter (2 region of interest) and over a large area (1 region of interest) containing both white and gray matter. The region-of-interest diameters were 1, 2, and 20 mm for the region of interest in the white, gray, and overall regions, respectively. The average and SD in the CBF values were calculated in each of the 12 regions of interest per section, resulting in 120 data points in all. Additionally, we also analyzed the results from some selected subscans from the set of 6 scans (3 scans, 2 scans, and 1 scan) to study whether CTP was feasible with fewer scans, which could potentially make the CTP imaging with the C-arm more viable clinically by reducing the x-ray and contrast dose as well as reducing the image-acquisition and processing time.

For each dataset, averages and SDs were calculated for each of the 12 region of interest in the different hemispheres, tissue types, and injection protocols. The Bland-Altman plots for average-versus-mean difference, the CCC (ρ) and the Pearson correlation coefficient (r) for a match between the left and right hemisphere CBF values on CT alone and the agreement between CT and C-arm CBCT data were also calculated. The CCC measures the exact match between values from the 2 systems, whereas the Pearson correlation coefficient tracks how well the values correlate with or change each other. The CBF maps acquired from the

clinical CT data were used as the gold standard for the calculations. All statistical analyses were done with STATA, Release 9.2 (StataCorp, College Station, Texas).

Results

The representative CBF maps in 1 of the animals are shown in Fig 2. The results from different injections are compared between C-arm CBCT (top row) and clinical CT (bottom row). A qualitative analysis shows that the CBF values for the 2 imaging modalities have a similar range of values. The calculated CBF values from clinical CTP measurements ranged from 3.5 to 71.2 mL/100 g/min, with the average value ranging from 39.81 ± 11.96 to 49.80 ± 8.61 mL/100 mg/min for white matter and 13.43 ± 5.89 to 25.36 ± 14.47 mL/100 mg/min for gray matter. The lower values in the range were associated with the 6-mL/s 50% iodinated contrast injection, while the higher values were obtained for the 3-mL/s 67% iodinated contrast injection. There were significant effects of tissue type ($P < .001$) and injection method ($P < .001$). The average differences in the CBF values between the 2 hemispheres for gray and white matter, their SDs, and overall ρ and r values measured for the 3 injections for CT alone are shown in Table 1. Because the animals imaged were healthy adults, it is expected that the CBF values in the 2 hemispheres will have a close match. The highest correlation coefficients were obtained for the 6-mL/s 50% iodinated contrast injection.

The CBF maps calculated from some of the selected 3-scan, 2-scan, and single-scan protocols that had the most promising results are shown in Fig 3. For comparison, the CBF maps from an equivalent CT section and from the complete 6-scan dataset are also shown.

Bland-Altman plots for the CBF data from CT and C-arm CBCT images are shown in Fig 4. The gray matter data are shown as filled gray circles, and white matter, by empty circles. These plots show that, on average, the 6-mL/s 50% iodinated contrast-concentration injection resulted in the least spread about the zero mean and appeared to have a slight linear bias with a positive intercept value.

The ρ and r values for evaluating the match in CBF value between CBCT and CT show the best results for the 6-mL/s 50% concentration. Table 2 shows the results for the top 3 scan set choices for this injection protocol. The set A-B-C-D-E-F consists of the 6 complete scans, while B-D-F and A-D are subsets consisting of 3 and 2 scans, respectively. The difference in the ρ and r values implies an inherent bias in the results. This was also observed in the Bland-Altman plots shown in Fig 4. Once this is removed, the 2 correlation coefficients should be identical.

No significant changes in heart rate or pCO_2 level were observed when the animal was imaged on the 2 scanners. The average difference in heart rate was 5.48 ± 5.17 beats per minute, and in the pCO_2 value, it was 1.29 ± 6.18 mm of Hg.

Discussion

In the above study, we measured the CBF in the pig brain by using a C-arm CBCT and compared it with CBF measurements from the same animal acquired by using a conventional CT scanner. Although only the CBF maps have been shown, it is possible to calculate the corresponding CBV, MTT, TTP, and Tmax maps, which are all derived from the same measured TDCs that had been used for generating the CBF maps.[17,18] These parameters have not been measured in this study, though because they are derived from the CBF maps, the correlation between C-arm CBCT and clinical CT for these parameters is expected to be similar to that of the CBF maps. A more complete evaluation is currently underway to verify this.

The CBF maps from the C-arm CBCT data appear to be smoother than the CT results (Fig 3). This finding could be attributed to the various smoothing and interpolation steps involved in calculating the CBF from the C-arm CBCT data to overcome the low temporal sampling. The CT data are sufficiently sampled and hence do not require the temporal interpolation steps.

The results show that the C-arm CBCT perfusion maps compare well with the corresponding CT maps even for 6, 3, or 2 multisweep scan sequences. This similarity indicates that including perfusion imaging in the workflow for image-guided intervention in the management of stroke may be feasible. This can be further assisted by newer CBCT systems with faster rotation times of ~3 seconds (Artis Zeego, Siemens). The use of 2 scans translates to a lower dose of iodinated contrast agent (eg, 2 scans require 2×3 mL/s for 8 seconds = 48 mL of iodinated contrast at 100% contrast concentration) needed for imaging. In addition, it may be possible to investigate the perfusion imaging with the C-arm CBCT system by using an IV instead of an IA injection, where the injected volume could now be increased because only 2 injections would be needed. All of these studies were conducted on healthy animals. In ischemic models in which the flow is typically slower, this method should produce comparable or better results because of a greater likelihood of improved temporal sampling of the TDC.

For this study, we have only tested 2 different injection rates and dilutions. It could be possible to further optimize the injection for increased accuracy of the results. Also, we have used a simple step injection profile. However, the injector used allows programming of fairly arbitrary profile shapes if desired (this feature is currently available only for research purposes). Using an injection profile that is optimized for the best mixing of iodinated contrast with blood flow in the aortic arch could further improve the results.

In these studies, we have used an aortic arch injection to allow multiple iodinated contrast injections at lower volumes for greater image contrast in C-arm CBCT imaging. However, it should not be a barrier to adopting this technique clinically because patients will be undergoing arterial catheterization for their endovascular therapy. Hence, it does not change the treatment workflow.

As mentioned above, the flow of contrast into the 2 cerebral hemispheres is sensitive to the location of the catheter tip in the aortic arch. For this study, a DSA image was used to estimate qualitatively whether the iodinated contrast was flowing evenly in the 2 CCAs. More recently, we have developed an automated method for quantitative measurement to ensure even distribution of the iodinated contrast in the 2 arteries.[19] The first step involves automatic segmentation of the CCAs from DSA images. The average ratio of the area under the curve from pixels in equal lengths of the 2 arteries is then calculated. For the ideal location of the catheter tip, this ratio is 1. For 6 animals, including those from this study, the ratio for the final location was found to be 0.99 ± 0.14 (3-mL/s injection rate), and 1.10 ± 0.13 (6-mL/s injection rate).

In these studies, the higher injection rate resulted in better results. These could be attributed to better flow and improved mixing of the contrast agent into the carotid arteries and less loss of iodinated contrast into the subclavian arteries at the higher flow rates. The bias in the results for the higher flow rate could be a result of the various noise-smoothing and interpolation algorithms used in processing the C-arm CBCT data that is sensitive to the actual Hounsfield unit value in the image. However, if the overall systematic bias for a given injection protocol is known, it can be accounted for as a calibration factor in calculating the final numbers.

Also, in this study, we assumed that the physiologic response following the contrast injections was identical for all 3 injection protocols. The effect of the cardiac cycle that causes variations in the cerebral blood flow[20]was ignored. Due to hardware constraints, it was not possible to include cardiac-gated injection of contrast agents. Including features such as electrocardiogram triggering the start of the injection, as shown in a recent publication,[21] could improve the outcome. In future studies, this feature will also be included and all injections will start at the same cardiac phase to eliminate any effect of the cyclic cardiac output.

With respect to dose to the patient, the C-arm CBCT system was not optimized for dose reduction for these studies. Including modifications such as increased collimation and a head-specific bow-tie filter could potentially reduce the dose in C-arm CBCT imaging.

In this study, only healthy pigs were considered. It is expected that in case of acute ischemic stroke, the CBF values will be lower[22] than those in the healthy patient. This would correspond to slower tissue enhancement and hence a better opportunity to get good temporal sampling of the data. Further investigation is required to test the limits of the reproducibility of the CBF measurements for high-flow values.

Conclusions

In the above animal study, the set of 6 scans each with 6×4 second sweeps by using a C-arm CBCT resulted in CBF values that were well-correlated with CTP CBF values. Use of as few as 2 scans also resulted in well-correlated values. The 6-mL/s injection containing 50% iodinated contrast produced the best agreement for CBF values calculated from images obtained from C-arm CBCT and clinical CT. The above results indicate that using C-arm CBCT for cerebral perfusion imaging is clinically feasible.

Acknowledgments

ABBREVIATIONS

AIF	arterial input function
CBCT	conebeam CT

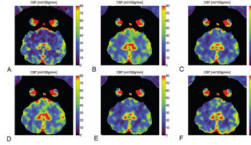|	
CBF	cerebral blood flow
CBV	cerebral blood volume
CCA	common carotid artery
CCC	concordance correlation coefficient
CTP	CT perfusion
MTT	mean transit time
DSA	digital subtraction angiography
DWI	diffusion-weighted images
FLAIR	fluid-attenuation inversion recovery
HCl	hydrchloric acid
IA	intra-arterial
IV	intravenous
pCO$_2$	end-tidal partial pressure of CO_2
PWI	perfusion-weighted imaging
ROI	region of interest
TDC	time-density curve
TTP	time to peak

References

1. Adams HP, del Zoppo G, Alberts MJ, et al. Guidelines for the early management of adults with ischemic stroke: a guideline from the American Heart Association/American Stroke Association Stroke Council, Clinical Cardiology Council, Cardiovascular Radiology and Stroke Council, Clinical Cardiology Council, Cardiovascular Radiology and Intervention Council, and the Atherosclerotic Peripheral Vascular Disease and Quality of Care Outcomes in Research Interdisciplinary Working Groups—the American Academy of Neurology affirms the value of this guideline as an educational tool for neurologists. Stroke. 2007; 38:1655–711. Epub 2007 Apr 12. [PubMed: 17431204]

2. Powers WJ, Zivin J. Magnetic resonance imaging in acute stroke: not ready for prime time. Neurology. 1998; 50:842–43. [PubMed: 9566357]

3. Albers GW, Thijs VN, Wechsler L, et al. Magnetic resonance imaging profiles predict clinical response to early reperfusion: the diffusion and perfusion imaging evaluation for understanding stroke evolution (DEFUSE) study. Ann Neurol. 2006; 60:508–17. [PubMed: 17066483]

4. McCarthy WJ, Park AE, Koushanpour E, et al. Carotid endarterectomy: lessons from intraoperative monitoring—a decade of experience. Ann Surg. 1996; 224:297–305. discussion 305–07. [PubMed: 8813258]

5. Reich DL, Hossain S, Krol M, et al. Predictors of hypotension after induction of general anesthesia. Anesth Analg. 2005; 101:622–28. [PubMed: 16115962]

6. Ahmed AS, Zellerhoff M, Strother CM, et al. C-Arm CT measurement of cerebral blood volume: an experimental study in canines. AJNR Am J Neuroradiol. 2009; 30:917–22. [PubMed: 19299488]

7. Bley T, Strother CM, Pulfer K, et al. C-arm CT measurement of cerebral blood volume in ischemic stroke: an experimental study in canines. AJNR Am J Neuroradiol. 2010; 31:536–40. [PubMed: 20053809]

8. de Lucas EM, Sanchez E, Gutierrez A, et al. CT protocol for acute stroke: tips and tricks for general radiologists. Radiographics. 2008; 28:1673–87. [PubMed: 18936029]

9. Wintermark M, Sincic R, Sridhar D, et al. Cerebral perfusion CT: technique and clinical applications. J Neuroradiol. 2008; 35:253–60. [PubMed: 18466974]

10. Kudo K, Sasaki M, Yamada K, et al. Differences in CT perfusion maps generated by different commercial software: quantitative analysis by using identical source data of acute stroke patients. Radiology. 2010; 254:200–09. [PubMed: 20032153]

11. Lieber BB, Sadasivan C, Hao Q, et al. The mixability of angiographic contrast with arterial blood. Med Phys. 2009; 36:5064–78. [PubMed: 19994517]

12. Fieselmann, A.; Ganguly, A.; Deuerling-Zheng, Y., et al. A dynamic reconstruction approach for cerebral blood flow quantification with an interventional C-arm CT. Proceedings of the 2010 IEEE International Symposium on Biomedical Imaging: From Nano to Micro; Rotterdam; the Netherlands. April 14–17; 2010. p. 53-56.

13. Montes, P. Dynamic Cone-beam Reconstruction for Perfusion Computed Tomography. Ruprecht-Karls-Universitat; Heidelberg, Germany: 2006. p. 165

14. Montes P, Lauritsch G. A temporal interpolation approach for dynamic reconstruction in perfusion CT. Med Phys. 2007; 34:3077–92. [PubMed: 17822015]

15. Marchal G. Automated multimodality image registration based on information theory. Inf Process Med Imaging. 1995:263–74.

16. Viola, P.; Wells, WM, III. Alignment by maximization of mutual information. In: Grimson, E.; Shafer, S.; Blake, A., et al., editors. Proceedings of the International Conference on Computer Vision; Los Alamitos; California. June 20–23; 1995. p. 16-23.

17. Østergaard L, Weisskoff RM, Chesler DA, et al. High resolution measurement of cerebral blood flow using intravascular tracer bolus passages. Part I. Mathematical approach and statistical analysis. Magn Reson Med. 1996; 36:715–25. [PubMed: 8916022]

18. Østergaard L, Sorensen AG, Kwong KK, et al. High resolution measurement of cerebral blood flow using intravascular tracer bolus passages. Part II. Experimental comparison and preliminary results. Magn Reson Med. 1996; 36:726–36. [PubMed: 8916023]

19. Fieselmann, A.; Ganguly, A.; Deuerling-Zheng, Y., et al. Automatic measurement of contrast bolus distribution in carotid arteries using a C-arm angiography system to support interventional perfusion imaging. Proceedings of the 2011 Society of Photographic Instrumentation Engineers Medical Imaging Conference; Lake Buena Vista; Florida. February 12–17; 2011.

20. McCulloch TJ, Turner MJ. The effects of hypocapnia and the cerebral autoregulatory response on cerebrovascular resistance and apparent zero flow pressure during isoflurane anesthesia. Anesth Analg. 2009; 108:1284–90. [PubMed: 19299801]

21. Badea CT, Johnston SM, Subashi E, et al. Lung perfusion imaging in small animals using 4D micro-CT at heartbeat temporal resolution. Med Phys. 2010; 37:54–62. [PubMed: 20175466]

22. Chalela JA, Alsop DC, Gonzalez-Atavales JB, et al. Magnetic resonance perfusion imaging in acute ischemic stroke using continuous arterial spin labeling. Stroke. 2000; 31:680–87. [PubMed: 10700504]
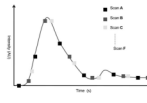
Fig 1.
Temporal spacing of different scan sets to allow higher temporal sampling. The function is a typical TDC extracted at 1-voxel position within a vessel, and the markers define the center time point of each rotation of the C-arm.

Fig 2.
CBF maps for 6-scan sets (A-B-C-D-E-F) from different injection-protocol C-arm CBCT (*A–C*) and CTP images (*D–F*). The 3 injection protocols used are 3 mL/s 67% (*A* and *D*), 6 mL/s 50% (*B* and *E*), and 3 mL/s 100% (*C* and *F*). All injections had a duration of 8 seconds.

Fig 3.
Results of CBF values for the 6-mL/s 50% contrast injection. *A–F*, CTP (*A*), C-arm CBCT (*B*) for scan sets A-B-C-D-E-F (*C*), B-D-F (*D*), A-C (*E*), and B-D (*F*) B.
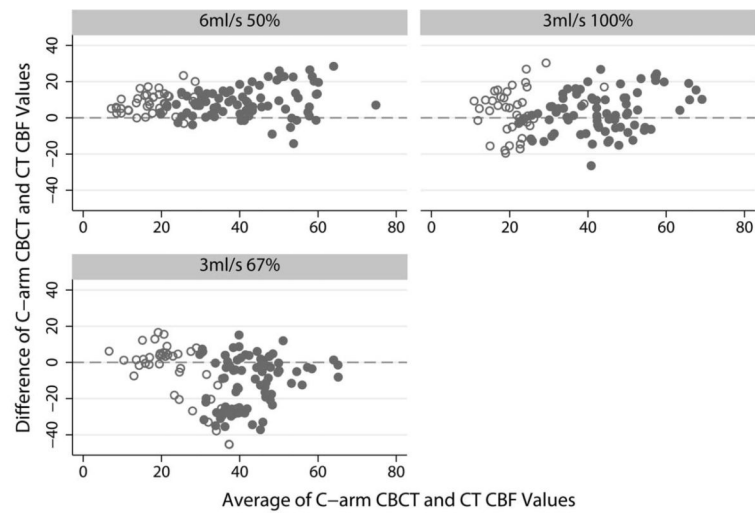
Fig 4.
Bland-Altman plots of C-arm CBCT versus CT CBF values for the 3 different injection protocols. Units for both axes are milliliters/100 g/min of tissue. Filled gray circles represent average values in gray matter regions of interest; and open circles, for white matter regions of interest.

Table 1

Difference in CBF between right and left hemispheres calculated from the clinical CT images only, for ROIs located in located in grey or white matter in the two hemispheres[a]

Injection Method	Difference in CBF between Left and Right Hemispheres (mL/100 g/min)	
	White Matter	**Grey Matter**
6 mL/s 50%		
Mean	2.04	1.98
SD	6.03	6.77
Overall ρ	0.92	
Overall r	0.92	
3 mL/s 100%		
Mean	0.75	0.26
SD	7.86	9.49
Overall ρ	0.84	
Overall r	0.84	
3 mL/s 67%		
Mean	0.73	0.61
SD	9.24	6.74
Overall ρ	0.90	
Overall r	0.90	

[a]Mean and SD values are given in milliliters/100 g/min. The overall CCCs and the Pearson correlation coefficients between the left and right hemispheres (without grey/white matter discrimination) are also included and were found to be identical, implying no underlying bias due to position of the catheter or otherwise.

Table 2

Statistical results comparing the CBF values from CT and CBCT from different scan sets for the 6-mL/s 50% contrast-concentration injection protocol[a]

Scan Set	CCC (ρ)	Correlation Coefficient (I)	Difference (CT-CBCT) (mL/100 g/min)		Bland-Altman 95% Limits
			Mean	SD	
B-D-F	0.796	0.87	6.56	8.34	−9.78—22.89
A-B-C-D-E-F	0.772	0.88	8.60	7.65	−6.40—23.59
A-C	0.751	0.88	8.78	7.68	−6.27—23.84

[a]The top 3 candidates are shown